Institute of Telecommunication Sciences and the National Bureau of Standards in various areas of communications, antenna research, propagation research, and system design. His present interests are in automated systems and automated network analyzers.

Cletus A. Hoer was born in Westphalia, MO in 1933. He attended Weber State College, Ogden, UT, and Sophia University, Tokyo, Japan, while serving in the U.S. Air Force from 1950 to 1954. He received the B.S. degree in engineering physics and the M.S. degree in electrical engineering, both from the University of Colorado, Boulder, in 1959 and 1967, respectively.

He joined the Boulder Laboratories, National Bureau of Standards, Boulder, CO, in 1956, where he was first engaged in developing instrumentation for measuring properties of magnetic materials at high frequencies. In 1962, he transferred to the High Frequency Impedance Standards Section, where he did research and development work on inductance standards, impedance bridges, inductive voltage dividers, attenuators, and directional couplers. In 1972, his emphasis shifted to developing Josephson junction detectors for precision RF attenuation measurements. Since 1974, he has been working on the theory and application of the 6-port concept to RF and microwave measurements. He and a coworker, Glenn Engen, received the Department of Commerce Gold Medal Award in 1976 for their development of the 6-port concept. He is the author or co-author of 36 technical papers and holds two patents.

Probing Electromagnetic Fields in Lossy Spheres and Cylinders

GARY H. WONG, STANISLAW S. STUCHLY, SENIOR MEMBER, IEEE, ANDRZEJ KRASZEWSKI, AND MARIA A. STUCHLY, SENIOR MEMBER, IEEE

Abstract—**Distributions of electric fields in lossy spheres and infinite lossy cylinders simulating biological objects were measured at 350, 920, and 2450 MHz. The measurements were performed in a computer-controlled scanning system using three different implantable nonperturbing probes. The results are compared with theory, and use of lossy spheres and cylinders for calibration of implantable probes is quantitatively evaluated.**

I. Introduction

DOSIMETRY OF electromagnetic fields is essential in quantifying biological effects of these fields and developing exposure standards for humans. Dosimetry is concerned with the determination of the electric-field intensity and the rate of energy deposition in biological bodies and their electrical models. The rate of energy deposition is defined as the specific absorption rate (SAR) usually expressed in W/kg [1]. The SAR is directly related to the intensity of the electric field *in situ* and the electric properties of the tissue.

Considerable progress in theoretical and experimental dosimetric methods has taken place in recent years, as reviewed elsewhere [1]–[3].

Lossy dielectric spheres serve as convenient models of biological bodies and their parts [1]–[3]. These models are relatively easy to analyze theoretically and to construct for experimentation. They also provide adequate simulation of some biological systems under certain exposure conditions [1].

The distribution of electric fields in a lossy sphere was previously obtained theoretically [4], and a computer program was developed [5]. Qualitative experimental verification was obtained [6]; however, a quantitative analysis of the accuracy with which the electric-field distribution can be measured by implantable electric-field probes is wanting. The SAR distribution was also measured by the thermographic technique [7].

The electric fields in lossy cylinders were determined analytically for an infinite cylinder [8] and analytically and experimentally for cylinders of finite length [9]. In the latter case, the experimental technique used had serious limitations when used for cylinders of small diameters

Manuscript received October 12, 1983; revised March 8, 1984. This work was supported in part by grants from the Natural Sciences and Engineering Research Council of Canada and the U.S. Office of Naval Research.

G. H. Wong, S. S. Stuchly, and A. Kraszewski are with the Department of Electrical Engineering, University of Ottawa, Ottawa, Ontario, Canada K1N 6N5.

M. A. Stuchly is with the Radiation Protection Bureau, Health and Welfare Canada, Ottawa, Ontario, Canada.

0018-9480/84/0800-0824$01.00 ©1984 IEEE

compared with the wavelength. This technique is also not acceptable for probing of the fields in biological bodies.

The purpose of this study was twofold, firstly, to evaluate the application of lossy spheres and cylinders for calibration of implantable probes used in bioeffects dosimetry, and secondly, to obtain quantitative experimental data and comparison with theoretical results at 350, 920, and 2450 MHz for the electric-field distribution in spheres and cylinders simulating the human body and its parts. This information can be further used for comparison with the electric-field distributions in models more closely resembling the human body.

II. Theoretical Analysis

A. Spherical Models

The electric-field and SAR distributions in lossy spheres irradiated by a plane wave were calculated using the Mie method [4]. The numerical calculations were obtained using a computer program provided courtesy of the Bureau of Devices and Radiological Health [5].

B. Cylindrical Model

The electric-field and SAR distributions in an infinite lossy cylindrical model were obtained under plane-wave irradiation. A recursive method, derived by Bussey and Richmond [8], was employed to solve the scattering amplitude of a lossy multilayered infinite cylinder for TE and TM modes as shown in Fig. 1. The infinite cylinder solution can be used to approximate a finite-length cylinder within a limited range of the cylinder length.

C. Limitations of the Numerical Techniques

Dimensions of the spherical and cylindrical models are restricted by the computational instability of the angular functions due to the arguments which are either too small or too large.

Restrictions of the program for the spherical model are as follows:

- the maximum number of layers is 10,
- each layer is homogeneous,
- $|k|r < 90.83$, where r is the radius of a homogeneous sphere and k is the propagation constant in the medium.

Limitations on the calculation for a homogeneous infinite cylinder are as follows:

- $|k|R < 22.8$,
- $|k|r > 1.87$, where R is the radius of the cylinder, r is the radius of the observation point, and k is the propagation constant in the medium.

III. Materials and Methods

A. Materials

Molds for the 6.6-cm, 12-cm, and 16-cm diameter spheres were made of 5-cm-thick RF transparent polystyrene foam. The mold for the 24.8-cm diameter cylinder of a length of 1.83 m was made of 3.2-mm-thick solid acrylic having a dielectric constant of 2.6.

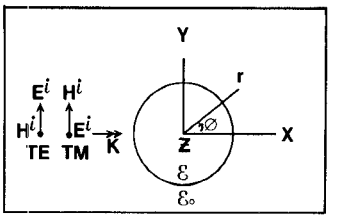

Fig. 1. TE and TM modes for a lossy circular infinite cylinder.

TABLE I
Sensitivities of the Implantable Probes Determined Using Various Models

f	Phantom	ϵ'	σ (S/m)	Sensitivity (μV per V^2/m^2) Holaday IME-01	EIT 979	Narda 2608
350 MHz	16-cm sphere	38.9	1.04	12±1	3.1±0.3	
	12-cm sphere				2 8±0 1	
	Cylinder, TM			18±1	2 4±0 1	
	Cylinder, TE			16±1	1.9±0.1	
	Slab			19±3	2.1±0.2	
920 MHz	16-cm sphere	76 0	1.58	72±5	)	0 71±0 06
	12-cm sphere			58±4	) 2 4±0 2	0.63±0.08
	6.6-cm sphere				)	0.71±0.04
	Slab			60±3	2 23±0.06	0.60±0.03
2.45 GHz	12-cm sphere	79	1 02			0 08±0 01
	6.6-cm sphere					0 08±0 02
	Slab					0.106±0.007

A semisolid phantom material which simulates the electrical properties of the average tissue was used at 350 MHz [10]. At frequencies of 920 MHz and 2.45 GHz, saline solutions were used as phantom materials because of their low viscosity, simplicity of preparation, and elimination of the mechanical perturbation of the phantom by the probe. The permittivities of different phantom materials, as measured by an automatic measurement system with an uncertainty of less than 3 percent [11], are given in Table I.

The electric-field intensities in different models were measured using a computer-based scanning system and an electric-field-probe technique [12].

The molds filled with phantom materials are placed in the far field of a selected antenna and accurately positioned to ensure a desired orientation of the incident electric field with respect to the scanning direction.

B. Probes

Three-dipole electric-field probes, a Narda Model 2608 (3 mm in diameter), an EIT model 979 (9 mm in diameter), and a Holaday Model IME-01 (19 mm in diameter), were used to measure the electric-field intensity. The characteristics of these probes are described elsewhere [13].

The sum of three voltages (V_T) detected by the diode-loaded dipoles is related to the square of the total electric-field intensity $|E_T|^2$ by the following expression:

$$V_T = B|E_T|^2$$

where B is the sensitivity of the probe in the tissue phantom material.

The sensitivity of each probe was determined for each model from the following expression:

$$B = \frac{\sum_{i=1}^{N} (V_T)_i \left(|E_T|^2\right)_i}{\sum_{i=1}^{N} \left(|E_T|^2\right)_i^2}$$

where $(V_T)_i$ is the total voltage at the probe detector diodes (a sum of the three voltages of the three dipoles), measured at an experimental point i, $(|E_T|^2)_i$ is the theoretical value of the internal electric-field intensity in the same point, and N is the number of points. The final value of the sensitivity was arrived at by an iterative process, in which only an unperturbed part of the distribution was included, i.e., that part for which the relative difference between the theoretical and experimental values was less than 10 percent.

C. System Uncertainties

There are several sources of errors in the system that may affect the accuracy of experimental results. Some of the errors can be limited to be negligibly small through proper arrangements and care. These include reflections from the walls and the scanning system. In this work, they have been eliminated by placing the whole system in an anechoic chamber and covering the frame of the scanning system with absorbing tiles. The incident electric field has to be well defined in terms of its amplitude and direction. The field intensity in our tests was determined from the antenna gain calibration and measurements of the input power to the antenna. The uncertainty in the intensity was estimated at ± 0.5 dB. The direction (alignment) of the antenna with respect to the probe was arranged within $\pm 1°$. The intensity of the field was always adjusted so that the probes operated in the linear region.

The main accuracy limitations in this experiment are due to the probes themselves, namely to the cross-coupling of the dipoles, lack of a perfectly isotropic response (due to small differences between the three dipole-diode assemblies), remnant pick-up of their high-resistance leads and the field perturbation by the leads.

IV. Results and Discussion

A. Spherical Models

A comparison of the theoretical and experimental data for a 16-cm diameter sphere at 350 MHz is shown in Fig. 2. On all illustrations, the probe is introduced from the positive z direction, while the wave is incident from the negative z direction. An excellent agreement can be seen for a smaller diameter probe (9 mm, EIT model), except at one end where the probe is introduced to the phantom. For a large-diameter probe (19 mm, Holaday model), significant deviations are also seen at the other end of the distance scanned. This is due to the smearing because of a poor spatial resolution of the probe.

The experimental error close to the point of probe entrance is due to a formation of a neck through which the phantom material is flowing outside the sphere.

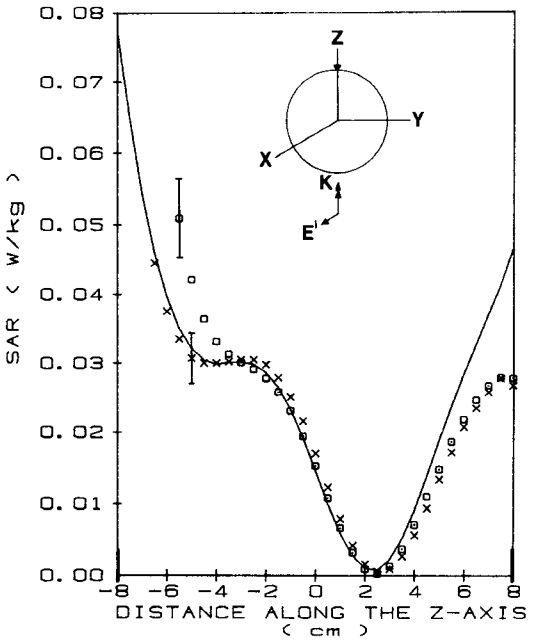

Fig. 2. Comparison of the calculated and measured SAR distribution along the z-axis of an average-tissue-phantom sphere. Solid line indicates the calculated values, $\times\times$ measured values with the EIT probe, □□ measured values with the Holaday probe. $\epsilon' = 38.9$, $\sigma = 1.04$ S/m, $f = 350$ MHz, Incident Power Density $= 1$ mW/cm^2, Diameter $= 16$ cm, Diameter/$\lambda_0 = 0.19$, Sensitivity $B = 3.1 \pm 0.3$ μV/(V^2/m^2) for the EIT probe and 12 ± 2 μV/(V^2/m^2) for the Holaday probe. The vertical bars show the uncertainty of measurements, the double arrow indicates the direction of incidence of the wave, and the single arrow shows the point where the probe is introduced into the phantom.

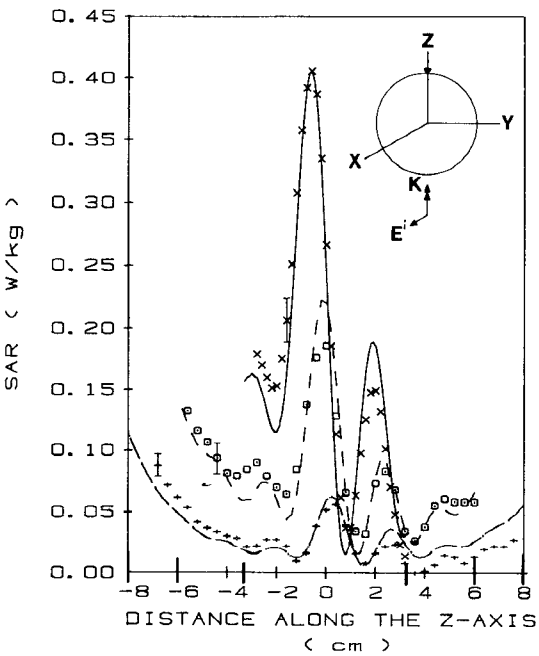

Fig. 3. Comparison of the calculated and measured SAR distributions along the z-axis for three spheres filled with the muscle-equivalent saline. $\epsilon' = 76.0$, $\sigma = 1.58$ S/m, $f = 920$ MHz, Incident Power Density $= 1$ mW/cm^2, Probe Narda. Solid line indicates the calculated values, $\times\times$ measured values for a sphere of a diameter $= 6.6$ cm, Diameter/$\lambda_0 = 0.2$, Sensitivity $B = 0.71 \pm 0.04$ μV/(V^2/m^2). Dashed line indicates the calculated values, □□ measured values for a sphere of a diameter $= 12$ cm, Diameter/$\lambda_0 = 0.37$, Sensitivity $B = 0.63 \pm 0.8$ μV/(V^2/m^2). The dash-dot line indicates the calculated values, $++$ measured values for a sphere of a diameter $= 16$ cm, Diameter/$\lambda_0 = 0.49$, Sensitivity $B = 0.71 \pm 0.06$ μV(V^2/m^2). The vertical bars indicate the uncertainty of measurements, the double arrow indicates the direction of incidence of the wave, and the single arrow shows the point of probe insertion.

Fig. 3 provides a comparison of theoretical and experimental results for three spheres at 920 MHz for the Narda probe. This is the smallest diameter (3 mm) probe, and smearing effect is very small. The "neck effect" is eliminated as a result of using a liquid phantom material.

Fig. 4 gives the results for 6.6-cm and 12-cm diameter spheres at 2.45 GHz as measured with the Narda and EIT probes. The spatial resolution limitations of both probes are apparent. For instance, for the 6.6-cm diameter sphere, where rapid changes of the SAR occur within about 1 cm, some smearing is evident in the second peak even for the Narda probe.

B. Cylindrical Model

Fig. 5 illustrates the data for the cylindrical model. The computational instability of the theoretical results close to the cylinder center was caused by the divergence of the Bessel functions in the region near the center.

The measurements were performed at the center of the cylinder and at a distance of 0.44 λ_0 from the end of the cylinder (points 1 and 3). Very good agreement was obtained for both probes for all locations except close to the point of the probe introduction. This was due to a small truncation of the cylinder.

C. General Discussion

As previously indicated, the agreement between theoretical and experimental SAR distributions is affected by several factors, e.g., limitations of the theoretical solution for the cylindrical model investigated, probe spatial resolution, model perturbation by the probe ("the neck" for semisolid phantom). Also, the agreement between the permittivity assumed in calculations and that of the material used plays a certain role.

The probe sensitivities as determined by a comparison of the experimental and theoretical SAR distributions in different models for the three probes at 350, 920, and 2450 MHz are summarized in Table I and compared with the data for slab phantoms [13]. A rather good agreement between the sensitivity values obtained using different models was obtained.

V. Conclusions

A quantitative comparison between the distributions of the specific absorption rate (SAR) obtained by analytical methods and by probing the electric fields in lossy spheres and cylinders using implantable probes was performed.

An excellent agreement between the theory and experiment was found within the limitations of the probes. The main limitations of the field probing are due to the spatial resolution of the probes, which in turn depends on the probe size. Other probe limitations include the probe symmetry, cross-coupling between the dipoles, and the field perturbation. The experiments confirmed that the computer-controlled experimental dosimetry system [12] allows to obtain the SAR distributions not only rapidly and conveniently, but that the accuracy is practically determined by the accuracy of the probe used, with much smaller errors due to the remaining parts of the system.

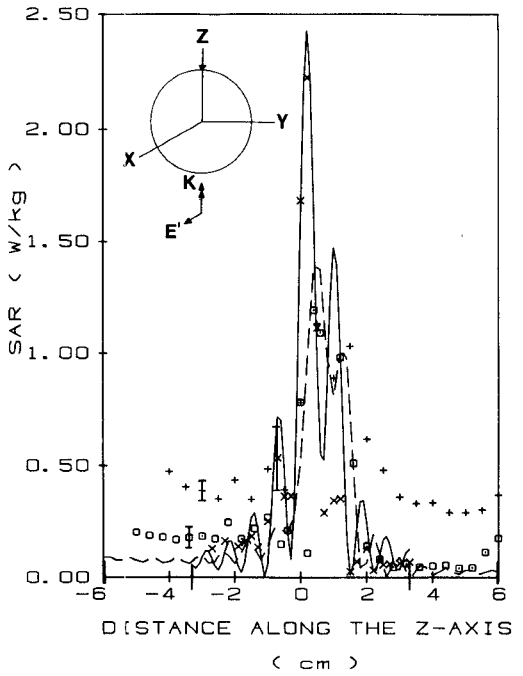

Fig. 4. Comparison of the calculated and measured SAR distributions along the z-axis for two saline-filled spheres. $\epsilon' = 77.9$, $\sigma = 1.02$ S/m, $f = 2.45$ GHz, Incident Power Density $= 1$ mW/cm^2. Solid line indicates the calculated values, $\times\times$ measured values with the Narda probe, Diameter $= 6.6$ cm, Diameter/$\lambda_0 = 0.54$, Sensitivity $B = 0.08 \pm 0.02$ μV/(V^2/m^2). Dashed line indicates the calculated values, □□ measured values with the Narda probe, + + measured values with the EIT probe, Diameter $= 12$ cm, Diameter/$\lambda_0 = 0.98$, Sensitivity $B = 0.08 \pm 0.01$ μV/(V^2/m^2) (Narda) and 0.10 ± 0.01 μV/(V^2/m^2) (EIT). The vertical bars show the uncertainty of measurements, the double arrow indicates the direction of the incidence of the wave, and the single arrow shows the point of probe insertion.

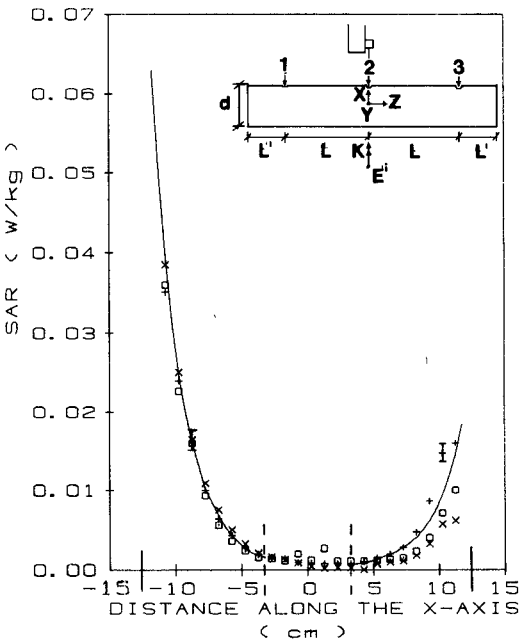

Fig. 5. Comparison of the calculated and measured SAR distribution across a circular cylinder filled with the average tissue phantom. $\epsilon' = 38.9$, $\epsilon'' = 53.5$, TE Mode, $f = 350$ MHz, Incident Power Density $= 1$ mW/cm^2, $L = 0.62$ λ_0, $L' = 0.44$ λ_0, $d = 0.29$ λ_0, Probe Holaday, Sensitivity $B = 16 \pm 1$ μV/(V^2/m^2). Solid line indicates the calculated values, + + measured values at 1, $\times\times$ measured values at 2, □□ measured values at 3. The vertical bars show the uncertainty of measurements; the double arrow indicates the direction of incidence of the wave.

Lossy dielectric spheres of proper sizes are convenient for calibration of implantable electric-field probes in tissue phantoms. They are superior to cylinders and slabs, as they facilitate calibration with the same or even better accuracy than cylinders and slabs, and are smaller in size. The size is of particular importance at lower frequencies (below 1 GHz) where the slab size required becomes cumbersome to handle [13].

ACKNOWLEDGMENT

The technical assistance of G. Hartsgrove and D. Adamski is greatfully acknowledged.

REFERENCES

[1] C. H. Durney, "Electromagnetic dosimetry for models of humans and animals: A review of theoretical and numerical techniques," *Proc. IEEE*, vol. 68, pp. 33–40, 1981.
[2] O. P. Gandhi, "State of the knowledge for electromagnetic absorbed dose in man and animals," *Proc. IEEE*, vol. 68, pp. 24–39, 1981.
[3] ——, "Biological effects and medical applications of RF electromagnetic fields," *IEEE Trans. Microwave Theory Tech.*, vol. MTT-30, pp. 1831–1847, 1982.
[4] A. Shapiro, R. Lutomirski, and H. Yura, "Induced fields and heating within a cranial structure irradiated by an electromagnetic plane wave," *IEEE Trans. Microwave Theory Tech.*, vol. MTT-19, pp. 187–196, 1972.
[5] S. M. Neuder, "Electromagnetic fields in biological media, Part II —The SCAT program, multilayered spheres, theory & applications," BRH Rockville, MD. Publication, Aug. 1979.
[6] H. Bassen, P. Herchenroeder, A Cheung, and S. Neuder, "Evaluation of implantable electric field probe within finite simulated tissue," *Radio Sci.*, vol. 12, no. 6S, pp. 15–25, 1977.
[7] A. W. Guy, "Analyses of electromagnetic fields induced in biological tissues by thermographic studies on equivalent phantom models," *IEEE Trans. Microwave Theory Tech.*, vol. MTT-19, pp. 205–214, 1971.
[8] H. E. Bussey and J. H. Richmond, "Scattering by a lossy dielectric circular cylindrical multilayer, numerical values," *IEEE Trans. Antennas Propagat.*, vol. AP-23, pp. 723–725, Sept. 1975.
[9] R. Bansai, R. W. P. King, and T. T. Wu, "The measurement of the electric field inside a finite dielectric cylinder illuminated by a plane wave," *IEEE Trans. Microwave Theory Tech.*, vol. MTT-30, pp. 1282–1285, 1982.
[10] C. H. Durney *et al.*, *Radiofrequency Radiation Dosimetry Handbook*, Second Ed. 1978, pp. 48–61.
[11] A. Kraszewski, M. A. Stuchly, and S. S. Stuchly, "ANA calibration method for measurement of dielectric properties," *IEEE Trans. Instrum. Meas.*, vol. IM-32, no. 2, pp. 385–387, 1983.
[12] S. S. Stuchly, M. Barski, B. Tam, G. Harstgrove, and S. Symons, "A computer based scanning system for electromagnetic dosimetry," *Rev. Sci. Instr.*, vol. 54, no. 11, pp. 1547–1550, 1983.
[13] M. A. Stuchly, A Kraszewski, and S. S. Stuchly, "Implantable electric field probe—Some performance characteristics," presented at the 5th Ann. Conf. of Bioelectromagnetic Society, Boulder, CO, June 12–17, 1983.

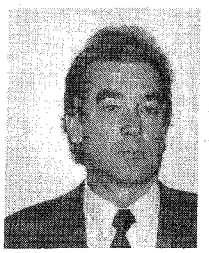

Gary H. Wong, photo and biography not available at time of publication.

Andrzej Kraszewski was born in Poznań, Poland, on April 22, 1933. He received the M.Sc. degree in electrical engineering from the Technical University of Warsaw, Warsaw, Poland, in 1958, and the D.Sc. degree in technical sciences from the Polish Academy of Sciences, (PAN), Warsaw, in 1973.

Beginning in 1953, he was employed at the Telecommunication Institute, Warsaw, in the research and development of microwave components and systems. Beginning in 1963, he joined UNIPAN Scientific Instruments, a subsidiary of the Polish Academy of Sciences, as the Head of the Microwave Laboratory. Starting in 1972, he was Manager of the Microwave Department of WILMER Instruments and Measurements, a subsidiary of the Polish Academy of Sciences in Warsaw, where he co-developed microwave instruments for moisture-content measurements and control. Since November 1980, as a Visiting Professor at the University of Ottawa, Canada, he has been engaged in research of interactions between dielectrics and electromagnetic fields. He is the author of several books on microwave theory and techniques, has published more than 80 technical papers on the subject, and holds 18 patents. He received several professional awards, among them the State Prize in Science in 1980.

Dr. Kraszewski is a member of the International Microwave Power Institute, the Polish Electricians Association, and is a member of the Editorial Board of the *Journal of Microwave Power*.

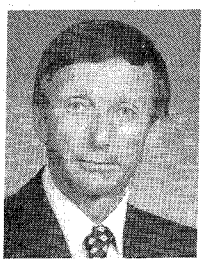

Stanisław S. Stuchly (M'70–SM'72) was born in Lwow, Poland, on November 20, 1931. He received the B.Sc. degree from the Technical University, Gliwice, Poland, and the M.Sc. degree from the Warsaw Technical University, both in electrical engineering, in 1953 and 1958, respectively, and the Ph.D. degree from the Polish Academy of Sciences, Warsaw, Poland, in 1968.

From 1953 to 1959, he was a Research Engineer in the Industrial Institute for Telecommunications, Warsaw, Poland. From 1959 to 1963, he was with the Warsaw Technical University. In 1963, he joined UNIPAN—Scientific Instruments, subsidiary of the Polish Academy of Sciences. From 1970 to 1976, he was with the University of Manitoba, Winnipeg, Canada. Since 1977, he has been with the University of Ottawa, Canada, where he is presently a Professor of Electrical Engineering.

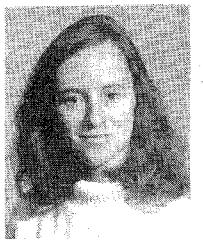

Maria A. Stuchly (M'71–SM'76) received the M.S. and Ph.D. degrees in electrical engineering from Warsaw Technical University and Polish Academy of Sciences in 1962 and 1970, respectively.

From 1962 to 1970, she was employed as a Senior R & D Engineer in a subsidiary of the Polish Academy of Sciences in Warsaw, Poland. Between 1970 and 1976, she was engaged in research in the field of microwave instrumentation and measurements, and microwave power applications at the Departments of Electrical Engineering and Food Science at the University of Manitoba. Since 1976, she has been with the Non-Ionizing Radiation Section, Radiation Protection Bureau, Health and Welfare Canada, where she is responsible for the development of microwave radiation protection standards and carries out research in the field of biological effects of microwave radiation. She is also nonresident Professor of electric engineering at the University of Ottawa.

Dr. Stuchly is a member of the Board of Directors of the Bioelectromagnetics Society and a member of IEEE Technical Committee of Man and Radiation.